

Range expansion shifts clonal interference patterns in evolving populations

Nikhil Krishnan¹ and Jacob G. Scott^{1,2,3}

¹Case Western Reserve University School of Medicine, Cleveland, OH, 44106, USA

²Translational Hematology Oncology Research and Radiation Oncology, Cleveland Clinic, Cleveland OH, 44106, USA

³Department of Physics, Case Western Reserve University, Cleveland, OH, 44106, USA

*npk13@case.edu, scottj10@ccf.org

ABSTRACT

The movement of a population through space can have profound impacts on its evolution, as observed theoretically, experimentally, and clinically. Furthermore, it has been observed that mutants emerging at the spreading front develop higher frequencies in the population than their counterparts further from the front. Here we use fundamental arguments from population genetics regarding expected time scales of beneficial mutant establishment and fixation in a population undergoing range expansion to characterize the degree of clonal interference expected in various regions while the population is migrating. By quantifying the degree of clonal interference along the wave front of a population undergoing range expansion using a measure we term the 'Clonal Interference Index', we show that evolution is increasingly mutation-limited toward the wave tip. In addition, we predict that the degree of clonal interference varies non-monotonically with respect to position along the wave front. The work presented here extends a powerful framework in population genetics to a canonical physical model of range expansion, which we hope allows for continued development of these models in both fields.

1 Introduction

2 It has been observed in a variety of clinical and experimental contexts that cell populations in a spatially complex
3 environment can rapidly adapt to selective pressures, including the presence of antibiotics¹⁻⁵. Theoretical work has
4 revealed how the spatial dynamics of population movement actively modulate evolutionary dynamics. Indeed, in
5 many circumstances, movement of a population to a new environment, or range expansion, drives population allele
6 frequencies from steady state⁶.

7 For example, it has been demonstrated that mutants arising closer to the front of the moving population during
8 range expansion carry a higher likelihood of fixing throughout the migrating population than in a well-mixed
9 population⁷⁻⁹. Further, range expansion can facilitate fixation of mutants that would otherwise not occur in a static
10 population^{6,10,11}. This can be observed in a canonical reaction-diffusion model of range-expansion (Box 1), which
11 models population movement in a wave-like manner. In this model, individuals at the front of the wave proliferate
12 faster than those that do not due to access to empty space¹². In addition, as the population continues to move,
13 the offspring of individuals at the wave front remain there and continue to exploit the empty space ahead of the
14 front. In this way, mutants arising at the wave front have enhanced proliferative capacity. Theoretical work on this
15 phenomenon, called mutation surfing, often in the context of an analogous stochastic model¹³, has shown that this
16 phenomenon occurs for deleterious, neutral, and beneficial mutations alike, underscoring the non-trivial impact of
17 range expansion on evolutionary dynamics^{8,14-16}.

18 We hypothesize that the observation that mutation surfing is less likely for a mutant arising from the wave bulk
19 than a mutant from the wave tip is due to an underlying, characterizable difference in evolutionary regime within
20 these regions of colonization. Insofar as beneficial mutations arising during range expansion are concerned, previous
21 work has been limited to the consideration of a wild type population capable of rare acquisition of a single mutation
22 granting a selective advantage^{15,16}.

23 In static populations, however, much of the foundational work in population genetics has provided powerful
24 frameworks for predicting the dynamics of evolving populations bearing multiple beneficial mutations^{17,18}. In such
25 populations, the dependence of the fate of beneficial mutants on population and selection characteristics has been
26 well described¹⁹⁻²¹. Beyond the limits of these models' constraints and their predictive power, this work has had
27 profound influence on our modern conceptualization and intuition about evolution. Here we seek to characterize
28 the evolutionary regimes experienced by a population undergoing range expansion that acquires multiple beneficial

29 mutation and displays clonal interference, or interactions between mutants while they fix. We achieve this by
 30 considering a stochastic Fisher wave with mutation describing such a population. We then quantify the likelihood
 31 of clonal interference by applying classical arguments regarding the population dynamics of beneficial mutations
 32 within the sub-population at each position using our Clonal Interference Index. Ultimately, we seek to build a global
 33 picture of evolutionary regime and the resulting clonal interference over range expansion space.

Box 1: Range Expansion Dynamics

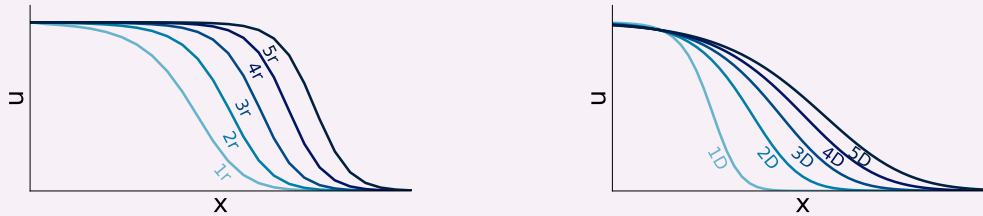
Fisher equation: 1D reaction-diffusion

$$\partial_t u = D\partial_x^2 u + ru(1-u) \quad (1)$$

where,

- $u(x, t)$ is the density of traveling particles as a function of position, x and time, t
- D is the diffusion constant
- r is the reaction rate

and at a given time r and D alter the wave profile in the following way respectively:



34

Results

35
 36 We begin by considering a deterministic description for reaction-diffusion of a bacterial population in one dimension
 37 (Box 1). Given an average growth rate of r and a maximum diffusion constant D_0 , we find that the maximum distance
 38 diffused within a generation is $\sqrt{D_0/r}$. We rescale position x by this distance to define a dimensionless position
 39 variable $\tilde{x} = x\sqrt{r/D_0}$. Population density $b(x, t)$ is scaled by its carrying capacity K : $\tilde{b} = b/K$, and the diffusion
 40 constant D by D_0 , the maximum diffusion constant: $\tilde{D} = D/D_0$ ²². Hereafter, we refer to these dimensionless
 41 parameters and variables without the tildes for notational convenience. We thus obtain the familiar Fisher's equation:
 42 $\partial_t b = D\partial_x^2 b + b(1-b)$ for change in population density with respect to time and position. With this description of
 43 range expansion we can introduce a beneficial mutation that arises with rate U_b and selective advantage $\alpha \equiv r_m/r_w$,
 44 where r_w is the average wild-type growth rate and r_m is the average mutant growth rate. Noting that at early times
 45 in a mutant's life and at small population sizes stochastic effects dominate, we have spatio-temporal dynamics for
 46 the wild-type (b) and mutant (b_m):

$$\partial_t b = D\partial_x^2 b + r_w b(1-(b+b_m)) - bU_b + \sqrt{\gamma_b(b)b(1-(b+b_m))}\eta(x, t), \text{ and} \quad (2)$$

$$\partial_t b_m = D\partial_x^2 b_m + r_m b_m(1-(b+b_m)) + bU_b + \sqrt{\gamma_{b_m}(b_m)b_m(1-(b+b_m))}\eta_m(x, t). \quad (3)$$

47 where $\eta(x, t)$ and $\eta_m(x, t)$ are Itô white noises satisfying $\langle \eta(x_1, t_1)\eta(x_2, t_2) \rangle = \delta(t_1 - t_2)\delta(x_1 - x_2)$, and $\gamma_b(b)$ and
 48 $\gamma_{b_m}(b_m)$ describe the magnitude of fluctuations for the wild-type and mutant waves respectively. It can be shown that
 49 $\gamma_b(b)$ and $\gamma_{b_m}(b_m)$ are determined by the sum of variance of birth and non-birth events divided by their co-variance
 50 for the wild-type and mutant populations respectively²³⁻²⁷. In other words, the strength of these fluctuations varies
 51 indirectly with population size, N , thus adding stochastic genetic drift effects to the deterministic Fisher equation.
 52 In this way, the choice of N , which depends on K , essentially determines the minimum density which is 'counted' in
 53 our simulations and gives compact support $[1/N, 1]$ in b and b_m . We will discuss the impact of this choice on the
 54 predicted fate of a beneficial mutant later.

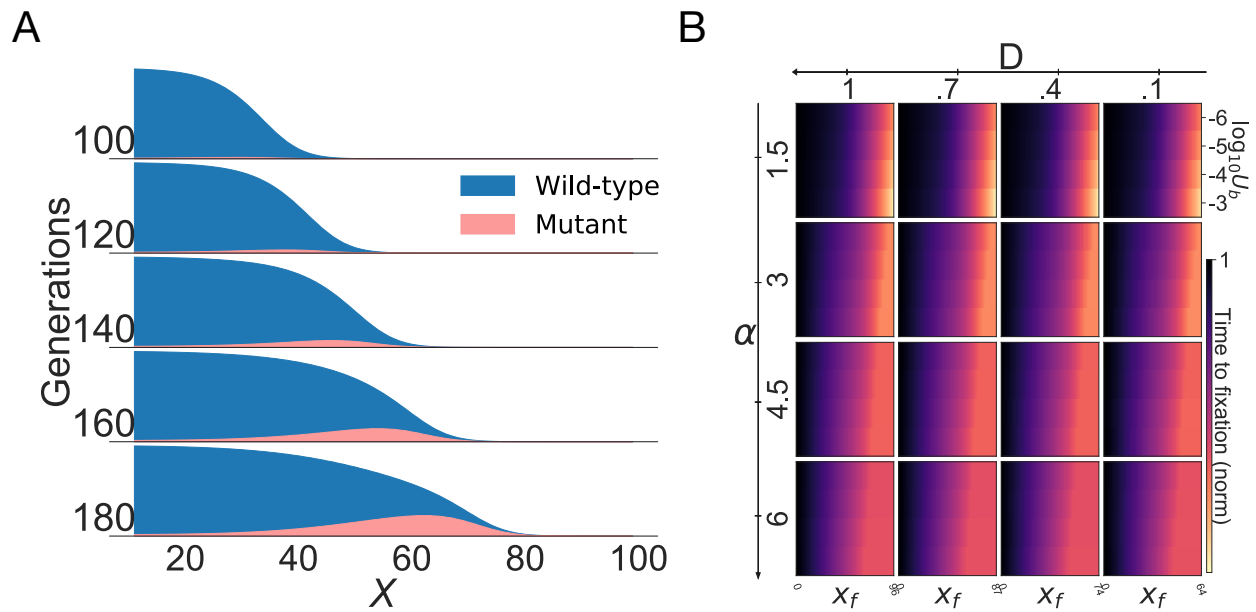


Figure 1. A: Balance between mutational supply and influence of genetic drift determines local mutant density. Wave profile during diffusive range expansion at various time points. Mutation rate $U_b = 10^{-3}$, selective advantage $\alpha = 1.5$, and diffusion constant $D = 0.4$. **B: Higher selective advantage and beneficial mutation rate decrease relative local fixation time toward the wave tip.** Simulated time to ‘local’ mutant fixation by position along wave front, x_f , over a range of mutation rates U_b , selective advantage α , and diffusion coefficients D

Simulation of equation (2) was initialized with a ‘Gaussian packet’ of wild-type cells of the form $\exp(-x^2/\sigma^2)$ where σ , which we set to 2, determines the shape of this packet²². We additionally set $r_w = 0.1$ and $N = 1 \times 10^7$. Simulating this one mutant reaction-diffusion system forward through time using an Euler-Maruyama scheme (Figure 1) reveals that at a given time before fixation throughout the wave front, the highest mutant frequency is seen at the very wave tip, while the highest absolute density is seen at a position further away from the tip, with diminishing mutant density behind this point. This pattern likely reflects the balance between mutational supply of a larger population away from the wave tip and enhanced stochastic effects toward the wave tip⁸.

We additionally measured the time for ‘local fixation’ at each position along the wave front. The wave front was defined by the initial wild-type wave profile which remains unchanged in the frame of reference traveling at the average velocity of the wave in the absence of mutants. Here, we introduce the concept of a ‘deme’, by which we examine a subpopulation of the wave along a length. In this way we conceptualize the cell in the context of Equations (2), (3), as a discrete number of individuals.

The number of individuals that define a deme of length $L \ll 1$ centered at a given position x with carrying capacity K as before is then $N = K \int_{x-L/2}^{x+L/2} b(x') dx'$. The average initial wave front profile, $b_i(x)$, then satisfies the following equation:

$$0 = D\partial_x^2 b_i + b_i r_w (1 - b_i) + v\partial_x b_i, \quad (4)$$

and is defined for all x where

$$K \int_{x-L/2}^{x+L/2} b(x') dx' > 1, \quad (5)$$

and otherwise is 0. The length of the wave front, L_f , is then defined by the maximum x for which b_i is defined as in Equations (4), (5). v is the average velocity of the wave front ($2\sqrt{Dr_w}$), as in the classic result for a Fisher (Kolmogorov–Petrovsky–Piskunov) wave. At any subsequent time after the initial wave profile has evolved, we

74 examine the wild-type wave front, recording the local fixation time as the time at which $K \int_{x_f-L/2}^{x_f+L/2} b(x'_f) dx'_f < 1$,
75 for every integer $x_f \leq L_f$ where x_f is position in the frame of reference travelling at the average velocity of the
76 initial wave front: $x_f = x - vt$ with v as above.

77 Predictably, increasing α and U_b causes mutations to reach local fixation in fewer generations along the entire
78 wave front (1B). By normalizing to the time to fixation at the beginning of the wave front we see that the *difference*
79 between the time to local fixation at the beginning at the wave front and at the wave tip is also increased with higher
80 selective advantage and mutation rate. The results here directly mirror the trend in mutant surfing probabilities
81 with respect to position shown by Lehe *et al.*¹⁵. Assuming mutants that fix throughout the population first take
82 over and surf at the wave front, local fixation at the wave tip earlier in time before regions further from the wave tip
83 as we observe in Figure 1 is a consequence of the increased mutant surfing probability near the tip of the expanding
84 population as previously established¹⁵.

85 However, as a single mutant population arises and survives long enough to surf along the front and eventually fix
86 throughout the front, subsequent mutational events may contribute to fixation of the mutant population. While Lehe
87 *et al.* phenomenologically correct for this when computing surfing probability with respect to position, assuming
88 it occurs rarely, the degree of this effect at various parameters and positions in the population undergoing range
89 expansion was not discussed.

90 While there has been limited description of beneficial mutants competing as they fix in a spatial context via game
91 theoretical models, the growth dynamics of such a population undergoing range expansion are poorly understood
92 [18, 28–30](#).

93 Though an analytic description of fixation times allowing for clonal interference is difficult even in a well-mixed
94 population, we can assess under what conditions and at what positions along the wave profile these considerations are
95 non-trivial. In the case of a well-mixed population, classic analysis has lended a framework by which to qualitatively
96 classify the extent of clonal interference in a well mixed-population (Box 2). Briefly one can derive an expression
97 for the average fixation time of a beneficial mutant that has not gone extinct and does not interact with another
98 growing clonal population, $\langle \tau_{fix} \rangle$. This is compared to the average expected time for a mutant that is destined to
99 eventually fix to arise in the population, or the average establishment time $\langle \tau_{est} \rangle$ ¹⁷.

100 When the average fixation time is far shorter than the average time for such a mutant to be established, the
101 population can be approximated as being isogenic with the fittest genotype available, termed strong selection weak
102 mutation (SSWM)^{17, 20}. When the aforementioned average fixation and establishment times become comparable,
103 separate mutant clonal populations will likely exist simultaneously, and compete with each other as the separate
104 clonal lineages grow¹⁸. The relative contributions of mutation rate and mutant fitness benefit underlying this behavior
105 is sometimes termed strong selection strong mutation (SSSM). As the establishment time becomes increasingly
106 short relative to fixation time, weak selection strong mutation (WSSM) takes places and many clonal populations
107 are expected to coexist at a time. As described in Box 2, $\langle \tau_{est} \rangle$ and $\langle \tau_{fix} \rangle$ are determined by N , U_b , and s ,
108 and the constraints on the above regimes can be stated in terms of these parameters, as is commonly seen in the
109 literature^{17, 18, 20, 31}.

110 While these regimes are theoretical simplifications, evidence indicates they each serve to simplify biologically
111 observable behavior^{32–34}. In kind, we can comment on the evolutionary regime of the local environment during
112 range expansion by a similar comparison of fixation and establishment times.

113 To find the expected establishment time, $\langle \tau_{est} \rangle$ of mutants with respect to position we must calculate the survival
114 probability of a single mutant arising at each position. We achieve this by assuming the survival probability, $u(x)$,
115 satisfies a backward Kolmogorov equation,

$$0 = \partial_x^2 u + ur_m(1 - b_i) - v\partial_x u - u^2, \quad (6)$$

Box 2: Population Genetics

Beneficial mutations in a well-mixed population :

For a large asexual population with fixed size N , and finite alleles conferring fitness advantage s , mutated between at rate U_b .

The average time for a single mutant that does not go extinct to fix on average, $\langle\tau_{fix}\rangle$, is:

$$\langle\tau_{fix}\rangle \approx \frac{1}{s} \log(Ns).$$

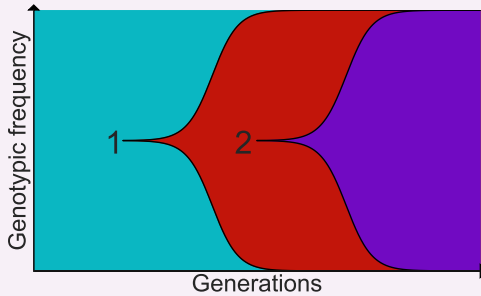
The average time for a mutant to arise and survive, $\langle\tau_{est}\rangle$, is

$$\langle\tau_{est}\rangle \approx 1/NU_b s.$$

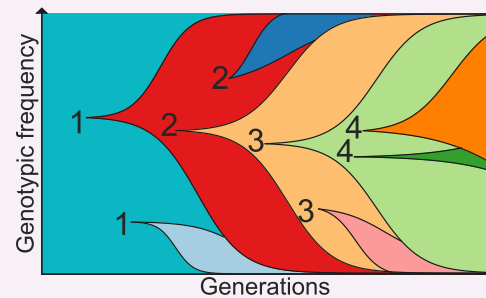
Dynamical regimes of beneficial mutations:

When $\langle\tau_{est}\rangle \gg \langle\tau_{fix}\rangle$ beneficial mutations fix ‘one at a time’ and at $t \geq \tau_{fix}$ the population is (on average) isogenic.

When mutants arise frequently enough relative to the fixation time to interfere with each other, or $\langle\tau_{est}\rangle < \langle\tau_{fix}\rangle$.



This regime is also known as the strong selection weak mutation (SSWM) regime, to highlight the *relative* strength of selection and mutation compared to each and other and N .



When $\langle\tau_{fix}\rangle$ is sufficiently larger than $\langle\tau_{est}\rangle$, the population is expected to always be polygenic, often termed the weak selection, strong mutation (WSSM) regime. When they are comparable, clones experience competition as they fix, termed strong selection strong mutation (SSSM)^{17, 18, 31}.

116

117 and saturates at $\sim r_m$ in the far reaches of the wave tip

118 Equations of the same form as Equation (6) classically have been used to describe a branching random walk^{15, 21}.
119 That it describes the survival probability of single beneficial mutant as a function of position is discussed further in
120 the Methods section.

121 We use Equation (6) to estimate the average establishment time, $\langle\tau_{est}\rangle$, of a mutant with respect to position
122 along wave front x_f as before. Given that mutants appear in the population at average rate U_b ,

$$\langle\tau_{est}\rangle \approx KU_b \int_{x_f - L/2}^{x_f + L/2} b(x'_f) u(x'_f) dx'_f \quad (7)$$

123

124 at a given x_f .

125 To find the average ‘local’ fixation time of a mutant that does not go extinct, we turn our attention again to the
126 wave front. A mutant arising in the wave front that does not go extinct will fix within its deme by diffusing from its
127 initial position in the frame of the wild-type wave to the wave tip where there are no wild-type individuals within
128 its deme, a distance $L_f - x_f$. It will then fix at x_f where it arose by surpassing the wild type wave front by an
129 additional distance $L_f - x_f$ (See Methods). We thus obtain:

$$\langle\tau_{fix}\rangle \approx \frac{L_f - x_f}{\sqrt{D}(\sqrt{r_m} - \sqrt{r_w})}. \quad (8)$$

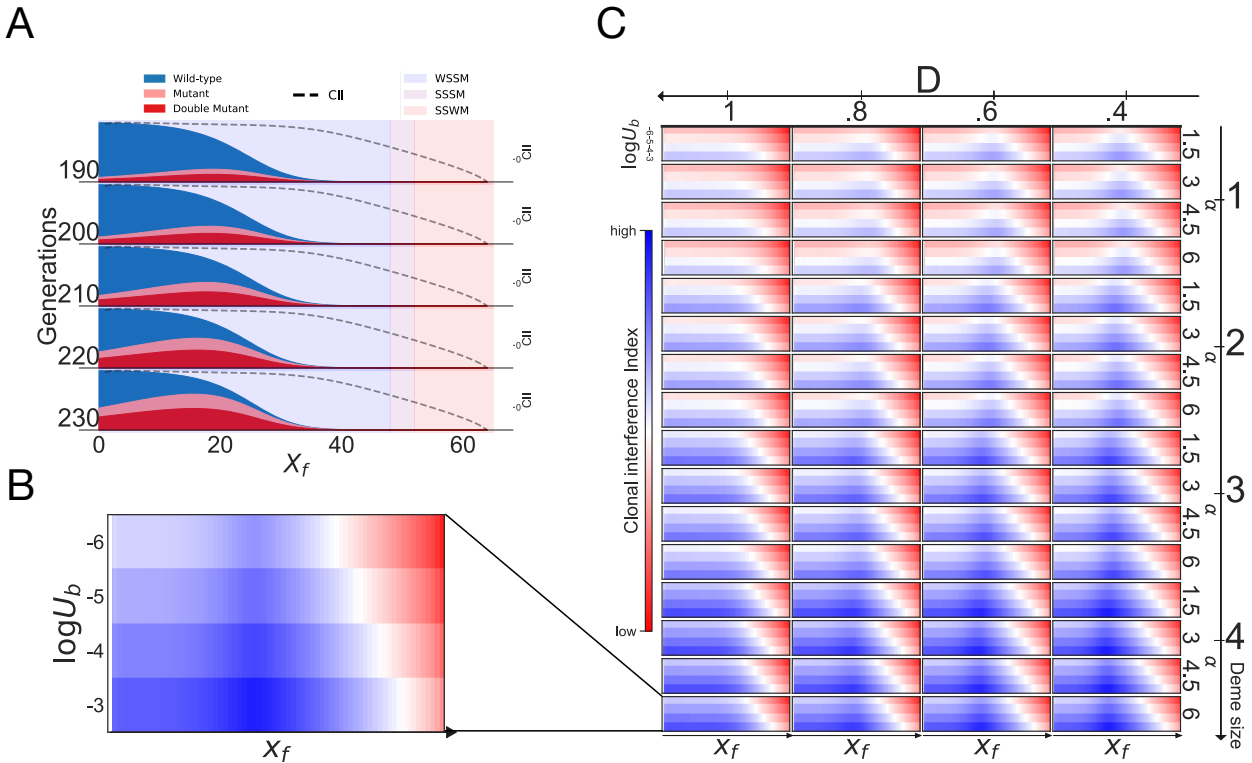


Figure 2. A: Clonal Interference Index predicts concurrent mutant and double mutant populations in wave bulk. Wave front of spreading population wave acquiring beneficial mutations at discrete time points with calculated Clonal Interference Index at each position, x_f on wave front. **B: The wave tip is less likely to display clonal interference.** CII at each position along wave front with varying U_b . **C: Smaller deme sizes and mutation rate decrease likelihood of observing clonal interference at a given position.** CII along wave front over a range of U_b , α , and D as we varied relative deme size.

130 To quantify the eco-evolutionary regime defined by the relative fixation and establishment times of a beneficial
 131 mutant at a given location we define the Clonal Interference Index (CII):

$$CII := \log(\tau_{fix}/\tau_{est}), \quad (9)$$

132 as calculated from Equations (6) - (8). Accordingly $CII > 0$ indicates that clonal interference is expected, and
 133 $CII \ll 0$, indicates that clonal interference is unlikely.

134 We evaluate the concordance of CII to simulated range expansion as before by simulating equations (2) and
 135 (3), but modified to allow for the development of up to five mutations, each with an identical additional selective
 136 advantage (α) compared to the clone with one less mutation following Desai *et al.*¹⁷. For the initial wave profile of
 137 the simulated wave satisfying Equations (4) - (5) as before, Equation (6) is numerically solved to find the $\langle\tau_{est}\rangle$ with
 138 Equation (7) at each position along the initial wild type wave profile. In addition $\langle\tau_{fix}\rangle$ for a mutant arising at x_f
 139 is calculated from Equation (8). Again, we note that these calculations be performed with varying deme size, which
 140 impacts $\langle\tau_{fix}\rangle$ by altering the length of the the wave front, and $\langle\tau_{fix}\rangle$ by altering the mutational supply available in
 141 each deme.

142 For a given wave profile, a deme size can be chosen such that the CII reflects a transition between eco-evolutionary
 143 regime along the wave profile relevant at times on the order of $\langle\tau_{fix}\rangle$ (Figure 2). Indeed, the appropriate choice of
 144 deme size for a given analysis depends on the specific question being asked, but as seen in Figure 2, this choice impacts
 145 the CII in intuitive ways. In general, the smaller the deme size, the faster the time for local fixation and the longer

146 the time for mutant establishment, resulting in a lower likelihood of clonal interference within a deme. Additionally,
147 model mutation rate predictably alters clonal interference index at a given deme size (Figure 2C). Specifically, with
148 a given (sufficiently high) α , the lower the U_b , the larger the portion of the wave with a low CII corresponding to
149 the SSWM regime. As a result of the structure of the expression used to estimate average establishment time, x_f
150 with maximum CII is $0 < x_f < L_f$ ¹⁷. Subsequently, we predict clonal interference is maximized at some position
151 between between the onset of the wave front and wave tip. This reflects the optimization of surfing probability and
152 population density $b(x_f)u(x_f)$ in Equation (9)¹⁵.

153 That CII is generally lower toward the front of the wave for a given deme size suggests that the same local
154 eco-evolutionary characteristics at the wave tip that yield the increased global fixation probabilities previously
155 observed give rise to mutation-limited dynamics when multiple mutations are allowed to occur^{1,15}. In accordance
156 with this observation, the eco-evolutionary dynamics that cause mutant fixation probability to decay away from the
157 tip give rise to increased clonal interference (Figure 2B).

158 Discussion

159 Our analysis shows how the relative balance of expected fixation and establishment times for a single mutant
160 arising from within a population undergoing range expansion modulate the extent of clonal interference expected
161 as a function of position. We show this by connecting canonical reaction-diffusion models of range expansion in
162 a population governed by accepted equations from population genetics capable of multiple beneficial mutations
163 which we assume to be of equal selective advantage. We present a clonal interference index as a way to quantify
164 the predicted clonal interference at each position as determined by a comparison of average local mutant fixation
165 and establishment times. Our results show that the evolutionary dynamics approach a mutation-limited regime
166 toward the wave tip during range expansion, and that clonal interference is maximized between the wave tip and the
167 onset of the wave front. In characterizing the local clonal interference likelihood of the population during range
168 expansion we learn about an essential influence on its evolutionary dynamics that persist if range expansion was no
169 longer occurring or took on a more complex form, such as reaction-diffusion-advection. In this way we present a
170 generalizable framework at the confluence of mathematical biology and population genetics allowing for analysis of
171 evolutionary regimes during range expansion.

172 Methods

173 Mutant fixing probability

As in the heuristic analysis of Lehe *et al.*, we begin by considering that the average wild-type wave front $b(x_f)$, in
the absence of mutants, which is stable through time. x_f is position in the frame of the wave front with velocity
 v : $x_f = x - vt$. From Equation (3) the average mutant density $\langle b_m(x_f, t) \rangle$ while the mutant population makes a
negligible contribution toward carrying capacity is as follows:

$$\partial_t b_m = D \partial_{x_f}^2 b_m + r_m b_m (1 - b). \quad (10)$$

174 If we imagine a mutant at time t and position x_f , the probability $\rho(x_f, t | X_f, T)$ of finding the mutant at some
175 short time later, T and some slightly different position X_f can be substituted into Equation (10) by assuming
176 $\rho(x_f, t | X_f, T) \approx \langle b_m(x_f, t) \rangle$,

$$\partial_t \rho = D \partial_{x_f}^2 \rho + r_m \rho (1 - b). \quad (11)$$

177 To find the probability of fixation $u(x_f)$ for a mutant arising from X_f we note the following:

$$u(X_f) = \int_{-\infty}^{\infty} \rho(x_f, t | X_f, T) u(x) dx, \quad (12)$$

178 as u essentially denotes the survival probability after a long time. Substituting Equation (11) into the time derivative
179 of (12), and integrating we obtain:

$$0 = \partial_x^2 u + u r_m (1 - b_i) - v \partial_x u. \quad (13)$$

180 Following Lehe *et al.*, we apply a u^2 correction term to obtain Equation (6) which yields a saturation of the
181 mutant probability at r_m in the critical branching process limit. This heuristic analysis is a useful intuitive framework
182 for the mutant fixation probability and more formally approximates the fixation probability as a solution of a
183 continuous backward Kolmogorov equation, the derivation of which can be found in standard texts, and has been
184 previously applied for approximating mutant surfing probabilities^{8,15}.

185 Mutant fixation time

186 For the wild type wave profile in the moving frame, we note that a mutant arising in the wave front takes over the
187 population upon surviving long enough to outpace the wild type wave front. Conditional on this survival, we note
188 that for a wave front of constant length L_f defined as in the Results section and mutant arising at x_f , the difference
189 $L_f - x_f$ is the distance the mutant must travel along the wave front where the wild-type population is decayed
190 below 1 and the mutant population has fixed within its deme.

191 In the frame of the wave front, ‘local’ fixation is defined as occurring when the mutant fixes at the position x_f
192 where it arose. This occurs once the mutant outpaces the wild type wave front and travels an additional distance
193 $L_f - x_f$ in the wild type frame, so that x_f is occupied by the fixing mutant front, and the wild type front has
194 now decayed below 1 here as well. Given the fixing mutant in the moving frame as velocity v_{m_f} and must travel a
195 distance $2(L_f - x_f)$, we find

$$\langle \tau_{fix} \rangle \approx 2 \frac{L_f - x_f}{v_{m_f}}. \quad (14)$$

196 We note the deterministic velocity of the mutant wave front in the frame traveling v_{m_f} is

$$v_{m_f} = 2(\sqrt{Dr_m} - \sqrt{Dr_w}), \quad (15)$$

197 from the average deterministic velocity of a Fisher wave. Thus, we obtain Equation (7),

$$\langle \tau_{fix} \rangle \approx \frac{L_f - x_f}{\sqrt{D}(\sqrt{r_m} - \sqrt{r_w})}.$$

198 References

- 199 1. Comins, H., Hassell, M. & May, R. The spatial dynamics of host–parasitoid systems. *J. Animal Ecol.* 735–748
200 (1992).
- 201 2. Markussen, T. *et al.* Environmental heterogeneity drives within-host diversification and evolution of *Pseudomonas*
202 *aeruginosa*. *MBio* 5, e01592–14 (2014).
- 203 3. Ciofu, O. & Tolker-Nielsen, T. Tolerance and resistance of *Pseudomonas aeruginosa* biofilms to antimicrobial
204 agents—how *P. aeruginosa* can escape antibiotics. *Front. microbiology* 10, 913 (2019).
- 205 4. Fusco, D., Gralka, M., Kayser, J., Anderson, A. & Hallatschek, O. Excess of mutational jackpot events in
206 expanding populations revealed by spatial Luria–Delbrück experiments. *Nat. communications* 7, 12760 (2016).
- 207 5. Baym, M. *et al.* Spatiotemporal microbial evolution on antibiotic landscapes. *Science* 353, 1147–1151 (2016).
- 208 6. Excoffier, L., Foll, M. & Petit, R. J. Genetic consequences of range expansions. *Annu. Rev. Ecol. Evol. Syst.* 40,
209 481–501 (2009).
- 210 7. Hallatschek, O., Hersen, P., Ramanathan, S. & Nelson, D. R. Genetic drift at expanding frontiers promotes
211 gene segregation. *Proc. Natl. Acad. Sci.* 104, 19926–19930 (2007).
- 212 8. Hallatschek, O. & Nelson, D. R. Gene surfing in expanding populations. *Theor. population biology* 73, 158–170
213 (2008).
- 214 9. Klopstein, S., Currat, M. & Excoffier, L. The fate of mutations surfing on the wave of a range expansion. *Mol.*
215 *biology evolution* 23, 482–490 (2005).
- 216 10. Edmonds, C. A., Lillie, A. S. & Cavalli-Sforza, L. L. Mutations arising in the wave front of an expanding
217 population. *Proc. Natl. Acad. Sci.* 101, 975–979 (2004).

- 218 **11.** Burton, O. & Travis, J. Landscape structure and boundary effects determine the fate of mutations occurring
219 during range expansions. *Heredity* **101**, 329 (2008).
- 220 **12.** Fisher, R. A. The wave of advance of advantageous genes. *Annals eugenics* **7**, 355–369 (1937).
- 221 **13.** Kimura, M. & Weiss, G. H. The stepping stone model of population structure and the decrease of genetic
222 correlation with distance. *Genetics* **49**, 561 (1964).
- 223 **14.** Travis, J. M. *et al.* Deleterious mutations can surf to high densities on the wave front of an expanding population.
224 *Mol. biology evolution* **24**, 2334–2343 (2007).
- 225 **15.** Lehe, R., Hallatschek, O. & Peliti, L. The rate of beneficial mutations surfing on the wave of a range expansion.
226 *PLoS computational biology* **8**, e1002447 (2012).
- 227 **16.** Farrell, F. D., Gralka, M., Hallatschek, O. & Waclaw, B. Mechanical interactions in bacterial colonies and the
228 surfing probability of beneficial mutations. *J. The Royal Soc. Interface* **14**, 20170073 (2017).
- 229 **17.** Desai, M. M. & Fisher, D. S. Beneficial mutation–selection balance and the effect of linkage on positive selection.
230 *Genetics* **176**, 1759–1798 (2007).
- 231 **18.** Sniegowski, P. D. & Gerrish, P. J. Beneficial mutations and the dynamics of adaptation in asexual populations.
232 *Philos. Transactions Royal Soc. B: Biol. Sci.* **365**, 1255–1263 (2010).
- 233 **19.** Haldane, J. B. S. A mathematical theory of natural and artificial selection, part v: selection and mutation. **23**,
234 838–844 (1927).
- 235 **20.** Gillespie, J. H. Molecular evolution over the mutational landscape. *Evolution* **38**, 1116–1129 (1984).
- 236 **21.** Kimura, M. & Ohta, T. Probability of gene fixation in an expanding finite population. *Proc. Natl. Acad. Sci.*
237 **71**, 3377–3379 (1974).
- 238 **22.** Croze, O. A., Ferguson, G. P., Cates, M. E. & Poon, W. C. Migration of chemotactic bacteria in soft agar: role
239 of gel concentration. *Biophys. journal* **101**, 525–534 (2011).
- 240 **23.** Doering, C. R., Mueller, C. & Smereka, P. Interacting particles, the stochastic fisher–kolmogorov–petrovsky–
241 piscounov equation, and duality. *Phys. A: Stat. Mech. its Appl.* **325**, 243–259 (2003).
- 242 **24.** Hallatschek, O. & Korolev, K. Fisher waves in the strong noise limit. *Phys. review letters* **103**, 108103 (2009).
- 243 **25.** Birzu, G., Hallatschek, O. & Korolev, K. S. Fluctuations uncover a distinct class of traveling waves. *Proc. Natl.*
244 *Acad. Sci.* **115**, E3645–E3654 (2018).
- 245 **26.** Gandhi, S. R., Yurtsev, E. A., Korolev, K. S. & Gore, J. Range expansions transition from pulled to pushed
246 waves as growth becomes more cooperative in an experimental microbial population. *Proc. Natl. Acad. Sci.*
247 **113**, 6922–6927 (2016).
- 248 **27.** Birzu, G., Matin, S., Hallatschek, O. & Korolev, K. S. Genetic drift in range expansions is very sensitive to
249 density feedback in dispersal and growth. *arXiv preprint arXiv:1903.11627* (2019).
- 250 **28.** Gerrish, P. J. & Lenski, R. E. The fate of competing beneficial mutations in an asexual population. *Genetica*
251 **102**, 127 (1998).
- 252 **29.** Kaznatcheev, A., Scott, J. G. & Basanta, D. Edge effects in game-theoretic dynamics of spatially structured
253 tumours. *J. The Royal Soc. Interface* **12**, 20150154 (2015).
- 254 **30.** Kaznatcheev, A., Peacock, J., Basanta, D., Marusyk, A. & Scott, J. G. Fibroblasts and alectinib switch the
255 evolutionary games played by non-small cell lung cancer. *Nat. ecology & evolution* **3**, 450 (2019).
- 256 **31.** Gillespie, J. H. Some properties of finite populations experiencing strong selection and weak mutation. *The Am.*
257 *Nat.* **121**, 691–708 (1983).
- 258 **32.** Joseph, S. B. & Hall, D. W. Spontaneous mutations in diploid *saccharomyces cerevisiae*: more beneficial than
259 expected. *Genetics* **168**, 1817–1825 (2004).
- 260 **33.** Drake, J. W. Avoiding dangerous missense: thermophiles display especially low mutation rates. *PLoS genetics*
261 **5**, e1000520 (2009).
- 262 **34.** Hao, D., Wang, L. & Di, L.-j. Distinct mutation accumulation rates among tissues determine the variation in
263 cancer risk. *Sci. reports* **6**, 19458 (2016).

264 **Acknowledgements**

265 The authors would like to thank Dr. Diana Fusco for her thoughtful feedback and discussion. JGS would like to
266 thank the NIH Loan Repayment Program for their generous support and the Paul Calabresi Career Development
267 Award for Clinical Oncology (NIH K12CA076917).

268 **Author contributions statement**

269 NK performed the mathematical analysis, wrote the code, performed the simulations, analyzed the data and wrote
270 the manuscript. JGS analyzed the data and wrote the manuscript.

271 **Code availability**

272 The code to perform the numerical simulations is available via github at [https://github.com/nkrishnan94/](https://github.com/nkrishnan94/Range-Expansion-Eco-Evo-Regime)
273 [Range-Expansion-Eco-Evo-Regime](https://github.com/nkrishnan94/Range-Expansion-Eco-Evo-Regime).